ECS Journal of Solid State
Science and Technology

Electric Current in Rate Equation for Parallel Plate Plasma-Enhanced Chemical Vapour Deposition of $SiC_xN_yO_z$ Film without Heat Assistance

To cite this article: Kenta Hori *et al* 2020 *ECS J. Solid State Sci. Technol.* **9** 024017

ECS Journal of Solid State Science and Technology, 2020 **9** 024017

Electric Current in Rate Equation for Parallel Plate Plasma-Enhanced Chemical Vapour Deposition of $SiC_xN_yO_z$ Film without Heat Assistance

Kenta Hori, Toru Watanabe, and Hitoshi Habuka[*,z]

Department of Chemistry Applications, Yokohama National University, Hodogaya, Yokohama 240-8501, Japan

A 50–500 nm-thick $SiC_xN_yO_z$ film was formed in parallel plate plasma at room temperature using a gas mixture of monomethylsilane, nitrogen and argon at 10−30 Pa for 5 min at the electric current of 1–16 mA. The film thickness and the concentrations of the silicon, carbon, nitrogen and oxygen were expressed by equations assuming that various chemical reactions in the gas phase and at the surface were enhanced by both the electric current and the partial pressure of the gases. The obtained equations showed the influence of the electric current on the film thickness and the compositions. Using the obtained equations, the existence and the extent of the deposition and the etching by the precursors and their combinations were evaluated.
 [DOI: 10.1149/2162-8777/ab7118]

Manuscript submitted November 25, 2019; revised manuscript received January 13, 2020. Published February 11, 2020.

Coating films made of various materials have been studied and formed on the surfaces of various tools and devices used in a corrosive environment.[1] There are various coating materials, such as silicon carbide (SiC), silicon nitride (SiN_x), silicon dioxide (SiO_2) and their mixtures, such as $SiC_xN_yO_z$.[1–3] In order to produce such coating films at low temperatures, the room temperature plasma enhanced chemical vapour deposition (PECVD) process has been studied.[4,5]

The PECVD process is considered to be influenced by various parameters, such as the partial gas pressures and electric current. Additionally, the precursors may interact with each other to cause the deposition and etching of the film. In order to enable a systematic study of the complicated process, the equations consisting of the partial pressures of the precursors and their cross terms were developed and evaluated in a previous study.[5] The obtained multi-term equations showed linear relationships between the experiment and calculation. Additionally, the role of each term was related to the deposition and etching.

While the electric current was fixed for simplification in the previous study,[5] it should be taken into account as one of the most influential factors. In this study for further development, the electric current was thus introduced to the equations for describing the thickness and the concentrations of the silicon, carbon, nitrogen and oxygen of the $SiC_xN_yO_z$ film, which was formed by the PECVD process without any heating assistance.

Experimental

In Fig. 1, the reactor and process used in this study are shown. The parallel plate plasma reactor (Soft Plasma Etcher-SE, Meiwafosis Co., Ltd., Tokyo, Japan.) has two 80 mm-diameter electrodes and two fluorocarbon resin parts. The electric current and total pressure are automatically measured and displayed in this reactor. A chamber is made of acrylic resin. The electrode distance between them is 62 mm, for the glow discharge. Typically, the plasma power was less than 0.36 W cm^{-2}. This reactor was similar to that used in previous studies.[4,5]

The substrate was a 10-mm wide and 10-mm long aluminum plate. The substrate was placed on the bottom electrode. The substrate surface was cleaned prior to the deposition, as shown in Fig. 1a, at 6 Pa and room temperature for 60 s. Next, in Step (B) shown in Fig. 1, the gas mixture of monomethylsilane (SiH_3CH_3, MMS) and nitrogen (N_2) at 5%–60% and 0%–80%, respectively, in ambient argon (Ar), was introduced into the chamber for 5 min. The total gas pressure was adjusted to 10–30 Pa. The electric current was 1–16 mA. The purities of monomethylsilane, argon and nitrogen gases were 99.9999%. The oxygen incorporation into the film can occur by the trace amount of O_2, H_2O, CO_2 and CO in the gases.

A scanning electron microscope (SEM) (VE-8800, Keyence, Tokyo) was used for evaluating the surface morphology. An X-ray photoelectron spectroscopy (XPS) (Quantera SXM, ULVAC-PHI Corp., Tokyo, Japan) measured the film thickness and chemical bonding state. The SEM and XPS data of the samples were reported in detail in the previous reports.[6,7] The center point of substrate was evaluated. Additionally, five substrates were simultaneously used for one film growth operation and were evaluated to confirm that there were not significant differences between the samples.

Overall Rate Process

Following the previous study,[5] the combinations of the simplified chemical reaction paths are preferred in order to obtain a simple and practical equation in contrast to the studies taking into account the many elemental reactions.[8–12]

For the parallel plate system, Fig. 2 is the assumption of the overall rate expressions. In the ambient plasma, the AB and C gases are activated and decomposed to produce the active species of A*, B* and C* along with the paths (a) in Fig. 2. Here, the active species contain various forms, such as ions, radicals, and fragments. At the same time, following paths (b) in Fig. 2, AB and C may collide with each other to produce the active species of A*, B* and C*. The A*, B* and C* go to the substrate surface that causes the deposition (+) and etching (−).

The rate equations of the overall reactions are assumed to be described by the consumption of the gases, following the reaction engineering.[13] The gas consumption is assumed to be proportional to the partial pressure, P_i, of the gas i and the electric current, I. The $k_{i\text{-}j\text{-}k}$ is the rate constant by the gases i, j and k. The positive and negative rate constants indicate the deposition and etching, respectively.

The argon, nitrogen and monomethylsilane are activated by Eqs. 1a, 2a and 3a, respectively. The Ar*, N*, C* and H* are expected to cause the deposition and etching. The overall rate, V, of Eqs. 1a, 2a and 3a are 1b, 2b and 3b, respectively.

$$\mathrm{Ar} \rightarrow \mathrm{Ar}^* \rightarrow \text{Deposition } (+) \text{ and etching } (-). \quad [1a]$$

$$V_1 = k_{\mathrm{Ar}} I\, P_{\mathrm{Ar}}. \quad [1b]$$

$$\mathrm{N_2} \rightarrow \mathrm{N}^* \rightarrow \text{Deposition } (+) \text{ and etching } (-). \quad [2a]$$

*Electrochemical Society Member.
[z]E-mail: habuka-hitoshi-ng@ynu.ac.jp

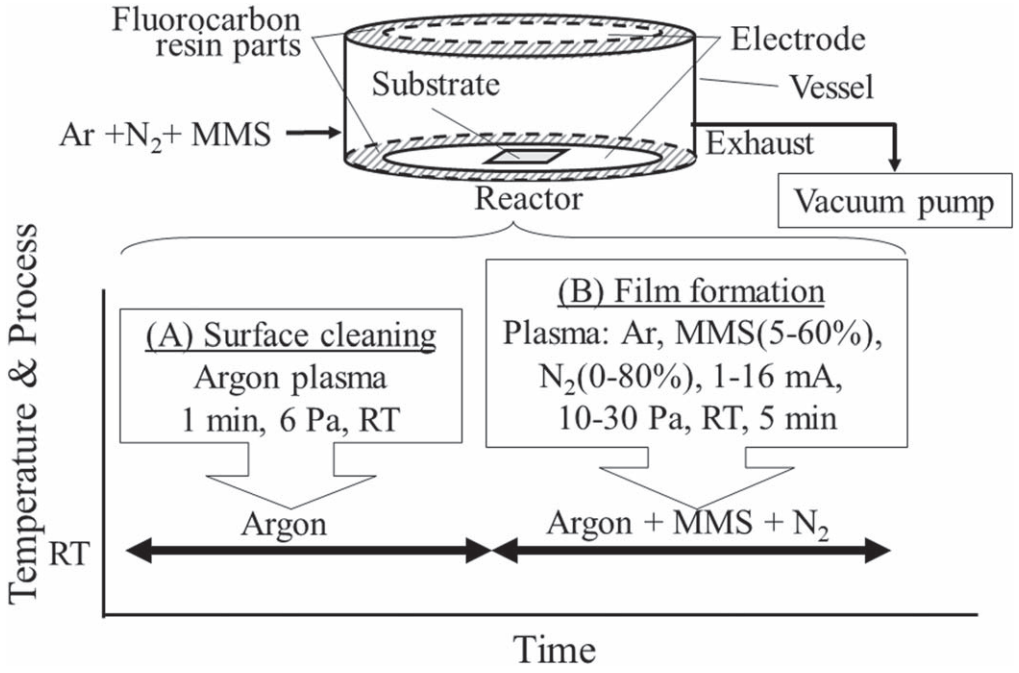

Figure 1. PECVD reactor and process in this study. (a) is the surface cleaning process using argon plasma, and (b) is the $SiC_xN_yO_z$ film deposition process using monomethylsilane, nitrogen and argon.

$$V_2 = k_{N2} I\, P_{N2}. \quad [2b]$$

$$SH_3CH_3 \rightarrow Si^*, C^* \text{ and } H^* \rightarrow \text{Deposition } (+) \text{ and etching } (-). \quad [3a]$$

$$V_3 = k_{SiH3CH3} I\, P_{SiH3CH3}. \quad [3b]$$

The chemical reactions between the gaseous species, indicated as paths (b) in Fig. 2, are taken into account. For example, the collisions of three gases, such as monomethylsilane, nitrogen and argon, produce the Ar*, N*, C* and H*. These are expected to contribute to the deposition and etching, which are expressed by Eqs. 4a, 5a, 6a and 7a. Their reaction rates are described by Eqs. 4b, 5b, 6b and 7b, respectively.

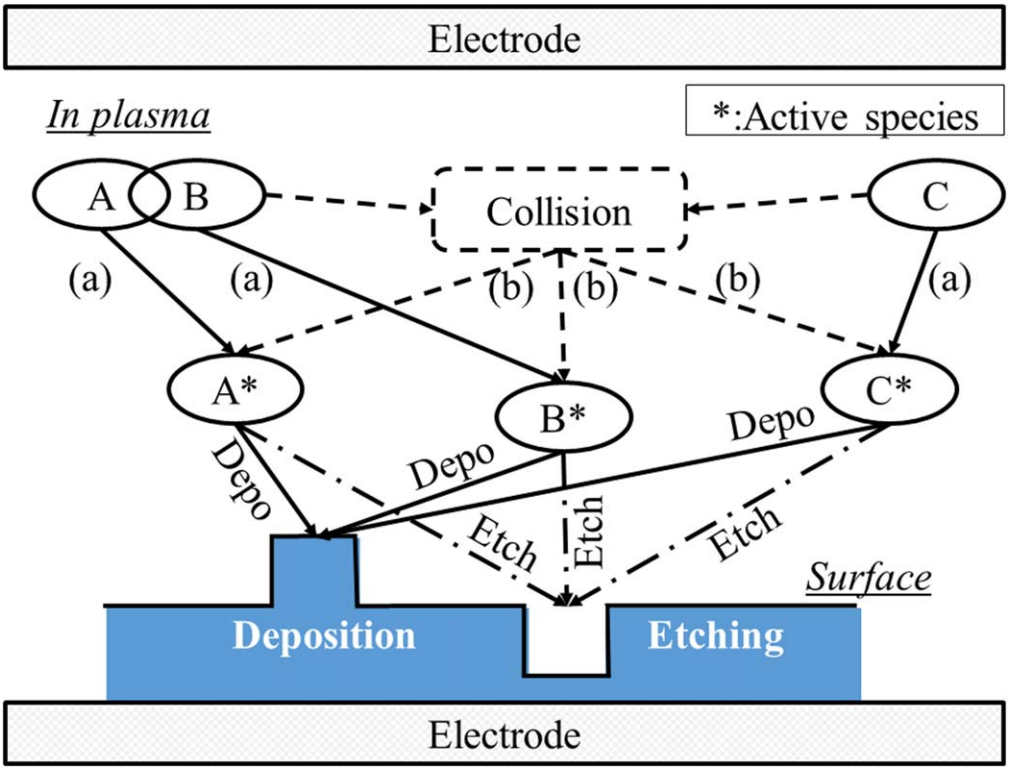

Figure 2. Reaction paths from gaseous species to deposition and etching at the surface and in the gas phase between two electrodes. (a): active species formation directly from the gases, (b): active species formation by the collision of the gases.

$$SiH_3CH_3 + Ar \rightarrow Si^*, C^*, H^* \text{ and } Ar^* \rightarrow \text{Deposition } (+) \text{ and Etching } (-). \quad [4a]$$

$$V_4 = k_{SiH3CH3-Ar}(I\ P_{SiH3CH3})(I\ P_{Ar}). \quad [4b]$$

$$SiH_3CH_3 + N_2 \rightarrow Si^*, C^*, H^* \text{ and } N^* \rightarrow \text{Deposition } (+) \text{ and Etching } (-). \quad [5a]$$

$$V_5 = k_{SiH3CH3-N2}(I\ P_{SiH3CH3})(I\ P_{N2}). \quad [5b]$$

$$N_2 + Ar \rightarrow N^* \text{ and } Ar^* \rightarrow \text{Deposition } (+) \text{ and Etching } (-). \quad [6a]$$

$$V_6 = k_{N2-Ar}(I\ P_{N2}I)(P_{Ar}). \quad [6b]$$

$$SiH_3CH_3 + N_2 + Ar \rightarrow Si^*, C^*, H^*, N^* \text{and } Ar^* \rightarrow \text{Deposition } (+) \text{ and Etching } (-). \quad [7a]$$

$$V_7 = k_{SiH3CH3-N2-Ar}(I\ P_{SiH3CH3})(I\ P_{N2})(I\ P_{Ar}). \quad [7b]$$

The total reaction rate $V_{Overall}$ is expressed as the summation of Eqs. 1b–7b.

$$\begin{aligned} V_{Overall} = {} & k_{Ar} I\ P_{Ar} + k_{N2} I\ P_{N2} + k_{SiH3CH3} I\ P_{SiH3CH3} \\ & + k_{SiH3CH3-Ar}\ I^2\ P_{SiH3CH3}\ P_{Ar} \\ & + k_{SiH3CH3-N2} I^2\ P_{SiH3CH3}\ P_{N2} + k_{N2-Ar} I^2\ P_{N2}\ P_{Ar} \\ & + k_{SiH3CH3-N2-Ar} I^3\ P_{SiH3CH3} P_{N2}\ P_{Ar}. \end{aligned} \quad [8]$$

The concentrations of silicon, nitrogen, carbon and oxygen in the film can be expressed in a form like Eq. 8. In order to obtain the rate constants in Eq. 8 for describing the film thickness and the concentrations of the silicon, carbon, nitrogen and oxygen by the least square approximation method, 14 data sets at the fixed film growth time of 5 min were used.

Results

Growth rate.—The linear relationship between the obtained film thickness and the film growth time in this study was confirmed prior to evaluating the PECVD process. Figure 3 shows that the film thickness increased with the increasing film growth time under one of the typical conditions. The concentrations of the monomethylsilane, nitrogen and argon were 40%, 40% and 20%, respectively; the total pressure was 15 Pa and the electric current was 1.0–1.3 mA. The obtained film thickness had a linear relationship with the film growth time. From the slope in this figure, the deposition rate was 17 nm min^{-1}.

Thickness and concentrations.—In order to express the thickness and the concentrations of the silicon, carbon, nitrogen and oxygen, the rate constants in the form of Eq. 8 were evaluated and shown by Eqs. 9–13 and in Figs. 4–8, respectively. The solid lines in the figures show the relationship when the calculation is equal to the measurement.

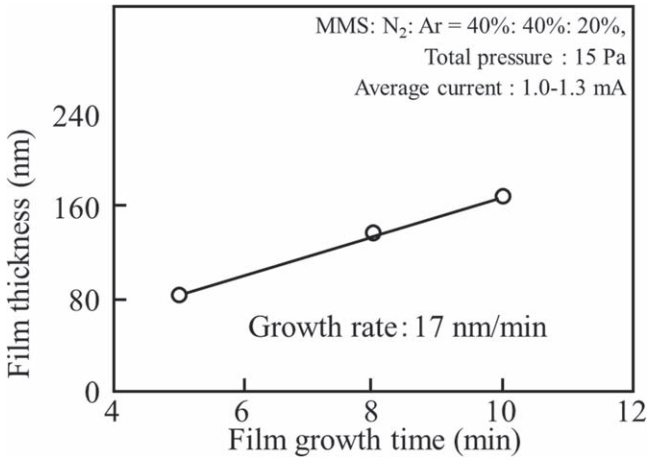

Figure 3. Film thickness vs film growth time.

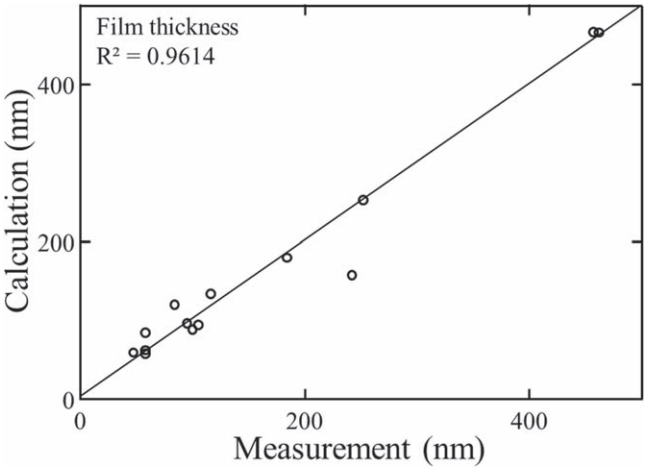

Figure 4. Correlation of the obtained film thickness between the measurements and calculations.

Film thickness:

$$\begin{aligned} \text{Thickness (nm)} = {} & 14.7I\ P_{SiH3CH3} - 1.27I\ P_{N2} + 4.70I\ P_{Ar} \\ & - 0.134I^2\ P_{SiH3CH3} P_{N2} \\ & - 0.650I^2\ P_{SiH3CH3} P_{Ar} - 0.0527I^2\ P_{Ar} P_{N2} \\ & + 0.0153I^3 P_{SiH3CH3} P_{N2} P_{Ar} + 12.0. \end{aligned} \quad [9]$$

Silicon concentration in the film:

$$\begin{aligned} \text{Silicon (\%)} = {} & 1.03I\ P_{SiH3CH3} - 0.179I\ P_{N2} + 0.233I\ P_{Ar} \\ & - 0.00521I^2 P_{SiH3CH3} P_{N2} \\ & - 0.0400I^2 P_{SiH3CH3} P_{Ar} + 0.00183I^2 P_{Ar} P_{N2} \\ & + 0.000454I^3 P_{SiH3CH3} P_{N2} P_{Ar} + 44.4. \end{aligned} \quad [10]$$

Carbon concentration in the film:

$$\begin{aligned} \text{Carbon (\%)} = {} & 1.67I\ P_{SiH3CH3} - 0.537I\ P_{N2} + 0.454I\ P_{Ar} \\ & + 0.00335I^2 P_{SiH3CH3} P_{N2} \\ & - 0.0743I^2 P_{SiH3CH3} P_{Ar} + 0.00902I^2 P_{Ar} P_{N2} \\ & + 0.000632I^3 P_{SiH3CH3} P_{N2} P_{Ar} + 18.3. \end{aligned} \quad [11]$$

Nitrogen concentration in the film:

$$\begin{aligned} \text{Nitrogen (\%)} = {} & 0.353I\ P_{SiH3CH3} - 0.213I\ P_{N2} + 0.220I\ P_{Ar} \\ & + 0.00861I^2 P_{SiH3CH3} P_{N2} \\ & - 0.0285I^2 P_{SiH3CH3} P_{Ar} + 0.004157I^2 P_{Ar} P_{N2} \\ & + 0.0000940I^3 P_{SiH3CH3} P_{N2} P_{Ar} + 8.10. \end{aligned} \quad [12]$$

Oxygen concentration in the film:

$$\begin{aligned} \text{Oxygen (\%)} = {} & -3.07I\ P_{SiH3CH3} + 0.828I\ P_{N2} - 0.929I\ P_{Ar} \\ & - 0.00251I^2 P_{SiH3CH3} P_{N2} \\ & + 0.142I^2 P_{SiH3CH3} P_{Ar} - 0.0124I^2 P_{Ar} P_{N2} \\ & - 0.00125I^3 P_{SiH3CH3} P_{N2} P_{Ar} + 29.6. \end{aligned} \quad [13]$$

The correlation coefficient was 0.96 for the film thickness in Fig. 4; those for the concentrations of silicon, carbon, nitrogen and oxygen in Figs. 5–8 were 0.77, 0.74, 0.63 and 0.83, respectively. Overall, the calculations could reproduce the typical trend of the experiments.

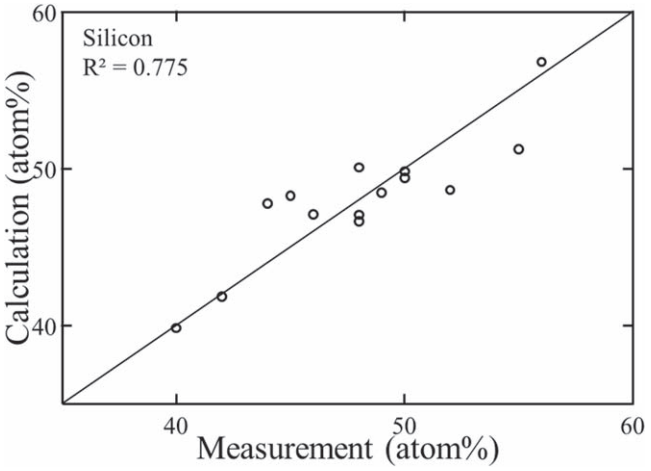

Figure 5. Correlation of silicon concentration in the obtained film between the measurements and calculations.

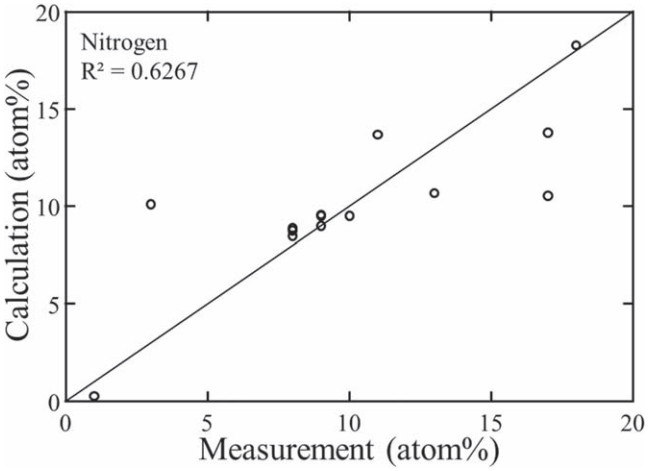

Figure 7. Correlation of film nitrogen concentration in the obtained film between the measurements and calculations.

Discussion

Electric current.—The influences of the electric current on the film thickness and various concentrations are shown in Figs. 9 and 10. Figure 9 shows the film thickness calculated at the partial pressures of the monomethylsilane, nitrogen and argon of 2, 7 and 9 Pa, respectively, for the film growth time of 5 min. At the increasing electric current from 1 to 10 mA, the film thickness is shown to non-linearly increase from 50 to 750 nm. While the film thickness increase between 1 and 5 mA is moderate, it becomes significant at higher than 6 mA. The non-linear film thickness increase at the higher electric current is considered to occur depending on the second and third order terms, such as $I^2 P_{SiH3CH3} P_{N2}$, $I^2 P_{SiH3CH3} P_{Ar}$, $I^2 P_{Ar} P_{N2}$ and $I^3 P_{SiH3CH3} P_{N2} P_{Ar}$, in Eq. 9.

The concentrations of silicon, carbon, nitrogen and oxygen were calculated at the various electric currents and shown in Fig. 10 assuming the same conditions as those in Fig. 9. The silicon concentration is expected to be nearly constant around 45%. Thus, it has a slight influence by the electric current. Additionally, the nitrogen concentration is considered to slightly increase at the electric currents between 1 and 10 mA. In contrast, the carbon concentration increases from 20 to 40% with the increasing electric current. In addition, the oxygen concentration is expected to significantly decrease with the increasing electric current.

Because the electric current was practically changed by adjusting the total pressure in the reactor shown in Fig. 1, the $SiC_xN_yO_z$ films were formed at the various total pressures by fixing the partial pressure ratio, for example, P_{SiH3H3}:P_{N2}:P_{Ar} = 1:4:10. Here, the major trend was assumed to be similar even if the conditions were slightly different from those in Figs. 9 and 10. The measurement is shown in Fig. 11, in which the electric current values corresponding to the total pressures are indicated. The electric current increased with the increasing total pressure. The relationship and the role of the total pressure and the electric current should be studied in the future work. Although both parameters seemed to change simultaneously correlating with each other, two parameters might have different chemical roles.

The obtained film thickness is shown in Fig. 11a. The film thickness increased with the increasing total pressure. Additionally, as shown in Fig. 11b, the silicon concentration was maintained at nearly 40%. While the carbon and nitrogen concentrations increased with the increasing total pressure, the increase in the nitrogen concentration was more moderate than that in carbon. The oxygen concentration decreased from 40% to 10% with the increasing total pressure. The overall trend shown in Fig. 11 agreed with those in Figs. 9 and 10. In conclusion, the equations in the form of Eq. 8 were applicable to design and obtain a film having the expected thickness and concentrations. The oxygen concentration may be controlled and adjusted by means of Eq. 13, while it might have been recognized as uncontrollable.

Precursors.—In order to understand which precursors and their interactions are active for the film deposition, the contribution ratio

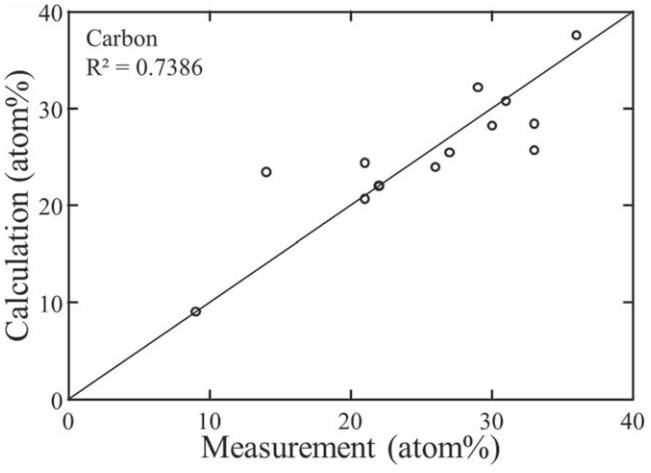

Figure 6. Correlation of carbon concentration in the obtained film between the measurements and calculations.

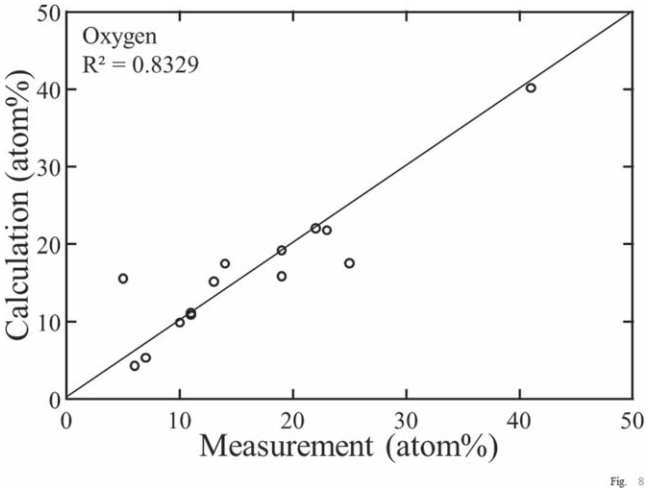

Figure 8. Correlation of oxygen concentration in the obtained film between the measurements and calculations.

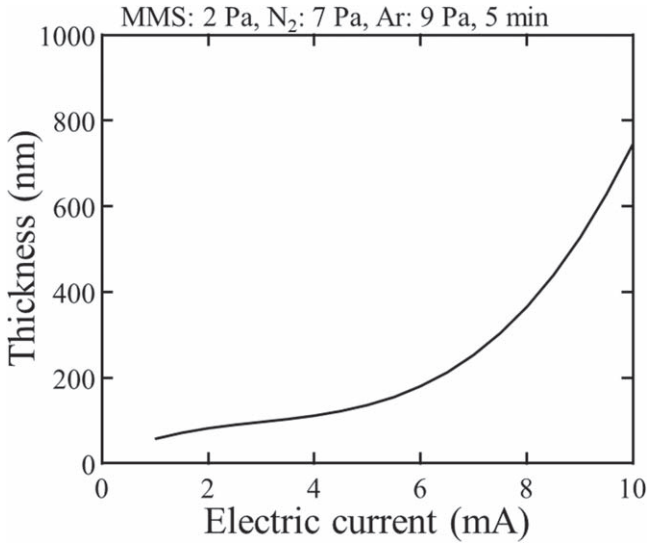

Figure 9. $SiC_xN_yO_z$ film thickness calculated at the various electric currents.

of each term in Eq. 9 is estimated at the electric current of 6 mA and shown in Fig. 12. In this figure, the values of the contribution are normalized using the highest value. The three positive terms of $IP_{SiH3CH3}$, IP_{Ar} and $I^3P_{SiH3CH3}P_{N2}P_{Ar}$ show a contribution to the deposition. The four negative terms of IP_{N2}, $I^2P_{SiH3CH3}P_{N2}$, $I^2P_{SiH3CH3}P_{Ar}$ and $I^2P_{Ar}P_{N2}$ can cause the etching. Assuming that the small contribution terms of IP_{N2}, $I^2P_{SiH3CH3}P_{N2}$ and $I^2P_{N2}P_{Ar}$ are negligible, a major part of the film deposition is considered to depend on $IP_{SiH3CH3}$, IP_{Ar} and $I^3P_{SiH3CH3}P_{N2}P_{Ar}$, while the etching by $I^2P_{SiH3CH3}P_{Ar}$ simultaneously occurred. When the partial pressures are fixed, the increase in the third order term of the electric current, such as $I^3P_{SiH3CH3}P_{N2}P_{Ar}$, is considered to be more significant than the increase in the second order term of $I^2P_{SiH3CH3}P_{Ar}$. Based on Fig. 12, the electric current is considered to accelerate the collisions between the three precursors of monomethylsilane, nitrogen and argon. Thus, the film thickness nonlinearly changes as shown in Fig. 9.

In addition to the film thickness, the concentrations of silicon, carbon, nitrogen and oxygen were studied from the viewpoint of their contribution to the deposition and etching. The roles of the precursors and their interactions were evaluated at the electric current of 6 mA using Eqs. 10–13 and shown in Figs. 13 and 14.

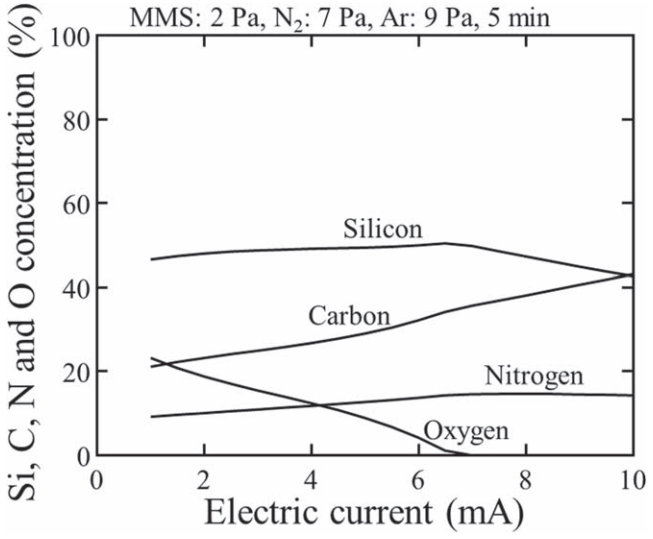

Figure 10. Concentrations of silicon, carbon, nitrogen and oxygen in $SiC_xN_yO_z$ film calculated at the various electric currents.

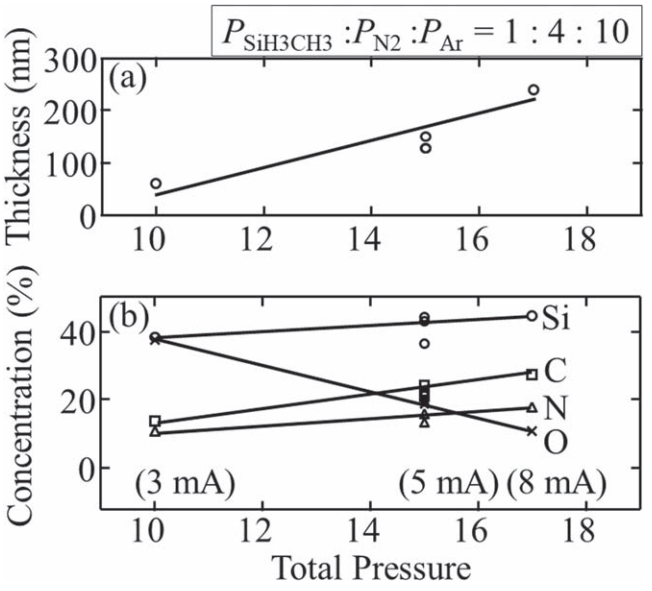

Figure 11. Measurement of (a) thickness and (b) concentrations of silicon, carbon, nitrogen and oxygen at the various total pressures. P_{SiH3H3}:P_{N2}:P_{Ar} = 1:4:10. The electric current values are denoted at the corresponding total pressures.

Similar to Fig. 12, the contribution values are normalized using the highest value in each figure.

Figure 13a shows the contributions of the terms in Eq. 10 for the silicon concentration. For the silicon incorporation, the four positive terms of $IP_{SiH3CH3}$, IP_{Ar}, $I^2P_{Ar}P_{N2}$ and $I^3P_{SiH3CH3}P_{N2}P_{Ar}$ affect the deposition, while the three negative terms of IP_{N2}, $I^2P_{SiH3CH3}P_{N2}$ and $I^2P_{SiH3CH3}P_{Ar}$ affect the etching. Among these, the major contributions of deposition by $IP_{SiH3CH3}$, IP_{Ar} and $I^3P_{SiH3CH3}P_{N2}P_{Ar}$ and that of etching by $I^2P_{SiH3CH3}P_{Ar}$ are the same as those for the film deposition in Fig. 12.

The contributions of the various terms in Eq. 11 to the carbon concentration are shown in Fig. 13b. While $I^2P_{SiH3CH3}P_{N2}$ has a low positive value different from Fig. 13a, the positive and negative contributions are entirely the same as those in Fig. 13a. Because the deposition contribution by $I^2P_{Ar}P_{N2}$ and $I^3P_{SiH3CH3}P_{N2}P_{Ar}$ increase

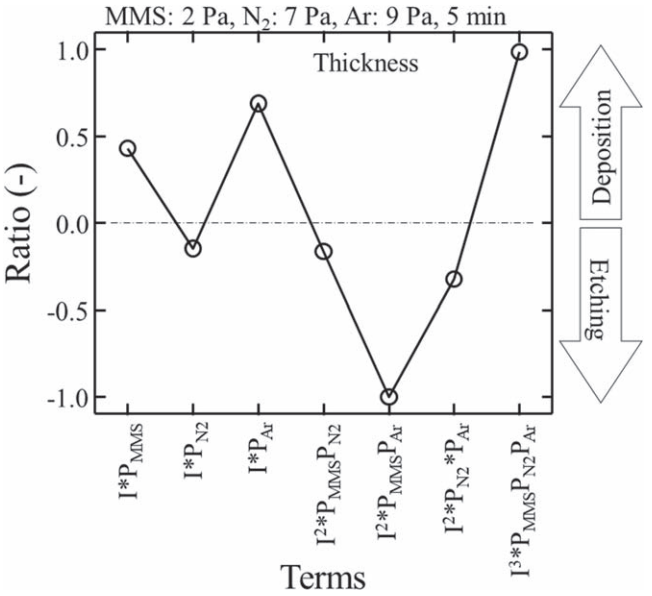

Figure 12. Contribution of various paths at 6 mA during the film formation process by deposition and etching.

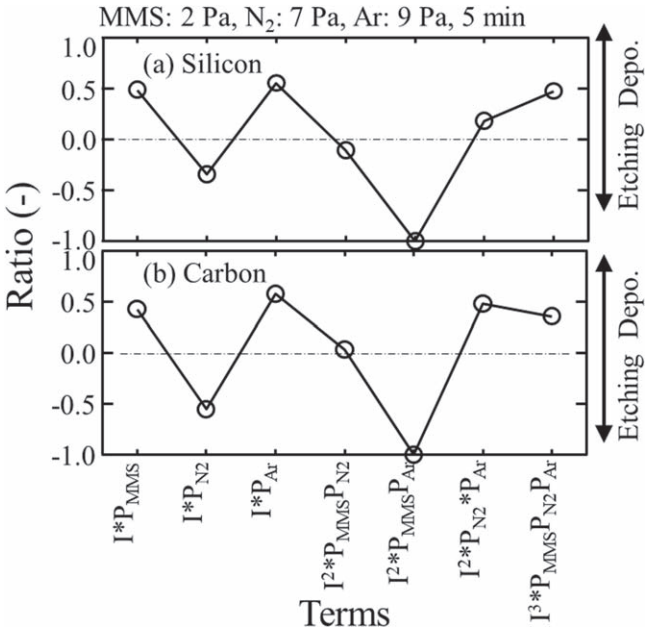

Figure 13. Contribution of various paths at 6 mA for incorporating (a) silicon and (b) carbon during the film formation process by deposition and etching.

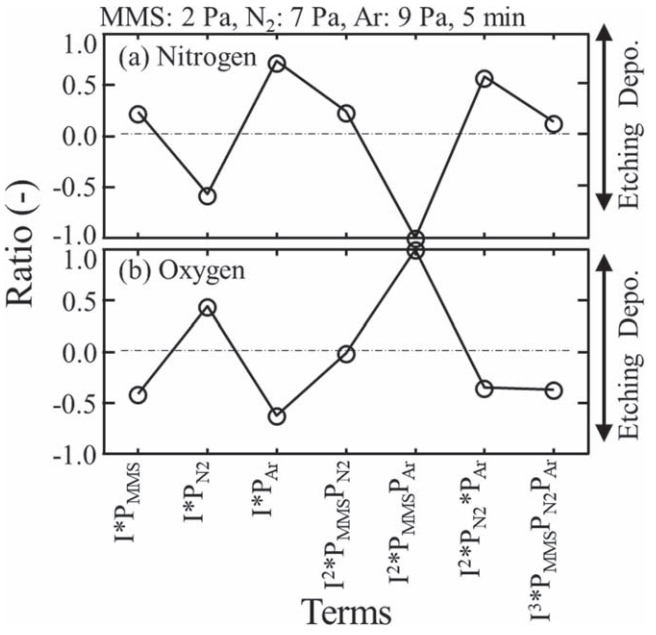

Figure 14. Contribution of various paths at 6 mA for incorporating (a) nitrogen and (b) oxygen during the film formation process by deposition and etching.

with the increasing electric current, the carbon concentration was evaluated to increase as shown in Fig. 10.

The contributions of the various terms in Eq. 12 to the nitrogen concentration are shown in Fig. 14a. The positive and negative contributions are entirely the same as those in Fig. 13. Because the nitrogen incorporation by $I^3P_{SiH3CH3}P_{N2}P_{Ar}$ is shown to be lower than $I^2P_{Ar}P_{N2}$, the increase in the nitrogen concentration is moderate with the increasing electric current.

In contrast, as shown in Fig. 14b, the oxygen incorporation is considered to occur by the contribution of the precursors opposite to those in Figs. 13 and 14a. The oxygen atoms are incorporated by the contributions of IP_{N2} and $I^2P_{SiH3CH3}P_{Ar}$, while they are removed by the contributions of $IP_{SiH3CH3}$, IP_{Ar}, $I^2P_{SiH3CH3}P_{N2}$, $I^2P_{Ar}P_{N2}$ and $I^3P_{SiH3CH3}P_{N2}P_{Ar}$. The summation of the etching contributions by $I^2P_{Ar}P_{N2}$ and $I^3P_{SiH3CH3}P_{N2}P_{Ar}$ is expected to become higher than the deposition contribution by $I^2P_{SiH3CH3}P_{Ar}$ with the increasing electric current.

Overall, the increase in the electric current was found to enhance the first, second and third order terms in Eq. 8. Their contribution to the concentrations of silicon, carbon and nitrogen is opposite to that of oxygen.

Conclusions

A $SiC_xN_yO_z$ film was formed in parallel plate plasma without any heating assistance using a gas mixture of monomethylsilane, nitrogen and argon at various electric currents. The film thickness and the concentrations of silicon, carbon, nitrogen and oxygen were described by the equations assuming that the rate of the various chemical reactions in the gas phase and at the surface was proportional to both the electric current between the electrodes and the gas partial pressures. The obtained equations showed the influence of the electric current on the film thickness and the compositions. Using the obtained equations, the role of the film formation and the etching caused by the gases and their combinations were evaluated. Overall, the increase in the electric current was evaluated to enhance all reactions in the PECVD reactor.

References

1. N. N. Greenwood and A. Earnshaw, in *Chemistry of the Elements* (Butterworth-Heinemann, Oxford, UK) 2nd ed. (1997).
2. A. S. Silva Sobrinho, M. Matreche, G. Crezemuszkin, J. E. Klemberg-Sapieha, and M. R. Wertheimer, "Transparent barrier coatings on polyethylene terephthalate by single- and dual-frequency plasma-enhanced chemical vapor deposition." *J. Vac. Sci. Technol. A*, **16**, 3190 (1998).
3. P. F. Carcia, R. S. Mclean, M. D. Groner, A. A. Dameron, and S. M. George, *J. Appl. Phys.*, **106**, 023533-1-6 (2009).
4. K. Shioda, M. Tanaka, A. Hirooka, and H. Habuka, "Non-heat assistance chemical vapor deposition of amorphous silicon carbide using monomethylsilane gas under Argon plasma." *Surf. Coat. Technol.*, **285**, 255 (2016).
5. M. H. Minh, T. Watanabe, K. Shioda, and H. Habuka, "Non-heat assistance plasma-enhanced chemical vapor deposition of SiCxNyOz film using monomethylsilane, Nitrogen and Argon." *ECS J. Solid State Sci. Technol.*, **6**, P443 (2017).
6. T. Watanabe, K. Hori, and H. Habuka, "Influence of metal and polymer substrate on $SiC_xN_yO_z$ film formation by non-heat assistance plasma-enhanced chemical vapor deposition using monomethylsilane, nitrogen and argon gases." *ECS J. Solid State Sci. Technol.*, **8**, 407 (2019).
7. T. Watanabe, K. Hori, and H. Habuka, "Anticorrosive behavior of $SiC_xN_yO_z$ film formed by non-heat assistance plasma-enhanced chemical vapor deposition using monomethylsilane, nitrogen and argon gases." *ECS J. Solid State Sci. Technol.*, **9**, 024001 (2020), (6 pages).
8. S. M. Sze, in *Semiconductor Devices* (John Wiley & Sons, New York, USA) 2nd ed., p. 378 (2002).
9. R. R. Tummala, in *Fundamentals of Microsystems Packaging* (McGraw-Hill, New York, USA) p. 582 (2001).
10. I. Hinkov, S. Farhat, C. P. Lungu, A. Gicquel, F. Silva, A. Mesbahi, O. Brinza, C. Porosnicu, and A. Anghel, "Microwave plasma enhanced chemical vapor deposition of carbon nanotubes." *J. Surf. Eng. Materi. Adv. Technol.*, **4**, 196 (2014).
11. A. L. Yarin, B. Rovagnati, F. Mashayeka, and T. Matsoukas, "A reaction model for plasma coating of nanoparticles by amorphous carbon layers." *J. Appl. Phys.*, **99**, 064310-1-12 (2006).
12. L. Pekker, "Simple model for calculating the rate constants of plasma-chemical reactions in low-pressure DC magnetron discharges." *Plasma Chem. Plasma Process.*, **18**, 181 (1998).
13. H. Scott Fogler, in *Essentials of Chemical Reaction Engineering* (Pearson Publisher, Inc., Boston, USA) (2011).